Supplementary Information

Reversible luminescent colour changes of mononuclear copper(I) complexes based on ligand exchange reactions by *N*-heteroaromatic vapours

Hiroki Ohara, Tomohiro Ogawa, Masaki Yoshida, Atsushi Kobayashi, Masako Kato*

Department of Chemistry, Faculty of Science, Hokkaido University, North-10 West-8, Kita-ku, Sapporo, Hokkaido 060-0810, Japan

Contents

Table S1. Energy, oscillator strength and major contribution of calculated transition for **3.**

Excited state	Energy / eV (nm)	Oscillator strength	Major contribution (%)
1	2.6227 (472.74)	0.0210	HOMO->LUMO (95)
			HOMO-1->LUMO (5)
2	2.6865 (461.51)	0.0024	HOMO-1->LUMO (96)
			HOMO->LUMO (4)
3	2.8444 (435.89)	0.0030	HOMO-2->LUMO (100)
4	3.0037 (412.77)	0.0010	HOMO->LUMO+1 (98)
			HOMO-1->LUMO+1 (2)
5	3.1141 (398.14)	0.0008	HOMO-1->LUMO+1 (98)
			HOMO->LUMO+1 (2)
6	3.2720 (378.92)	0.0024	HOMO-2>LUMO+1 (98)
			HOMO-4->LUMO+1 (2)
7	3.3695 (367.95)	0.0056	HOMO-4 ->LUMO (54)
			HOMO-3->LUMO (43)
			HOMO-2->LUMO (3)
8	3.4996 (354.28)	0.0251	HOMO-3->LUMO (57)
			HOMO-4->LUMO (43)
9	3.7799 (328.01)	0.0043	HOMO->LUMO+2 (86)
			HOMO-3->LUMO+1 (7)
			HOMO->LUMO+3 (4)
			HOMO-4->LUMO+1 (3)
10	3.7854 (327.53)	0.0006	HOMO-3->LUMO+1 (49)
			HOMO-4->LUMO+1 (38)
			HOMO->LUMO+2 (10)
			HOMO-2->LUMO+1 (3)

Table S2. Energy, oscillator strength and major contribution of calculated transition for **4**

Excited state	Energy / eV (nm)	Oscillator strength	Major contribution (%)
1	2.4954 (496.86)	0.0035	HOMO->LUMO (89)
			HOMO-1->LUMO (11)
2	2.5373 (488.64)	0.0133	HOMO-1->LUMO (86)
			HOMO->LUMO (10)
			HOMO-2->LUMO (4)
3	2.6800 (462.64)	0.0021	HOMO-2->LUMO (96)
			HOMO-1->LUMO (4)
4	3.2479 (381.73)	0.0021	HOMO-3->LUMO (92)
			HOMO-4->LUMO (5)
			HOMO-2->LUMO (3)
5	3.4677 (357.54)	0.0272	HOMO-4->LUMO (93)
			HOMO-3->LUMO (4)
			HOMO-1->LUMO+1 (3)
6	3.5156 (352.67)	0.0045	HOMO->LUMO+1 (96)
			HOMO-1->LUMO+1 (4)
7	3.5583 (348.44)	0.0029	HOMO-1 ->LUMO+1 (95)
			HOMO->LUMO+1 (5)
8	3.6982 (335.26)	0.0201	HOMO->LUMO+2 (100)
9	3.7241 (332.92	0.0001	HOMO-2->LUMO+1 (98)
			HOMO-1->LUMO+1 (2)
10	3.7526 (330.40)	0.0083	HOMO-1->LUMO+2 (97)
			HOMO->LUMO+4 (3)

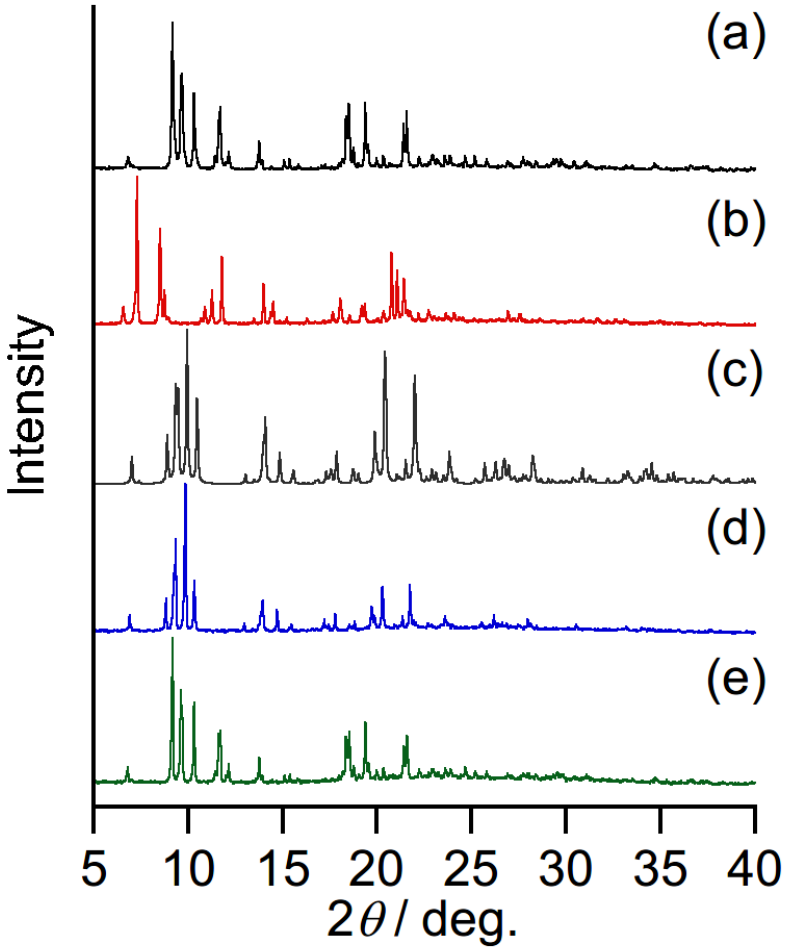

Fig. S1. Reversible PXRD pattern changes of complex **1** by pym vapour: (a) PXRD pattern of complex **1**, and (b) that after pym vapour exposure. (c) PXRD pattern of the sample after drying of the sample (b) under vacuum. (d) The simulation pattern of complex **3**, and (e) PXRD pattern after exposing the sample (d) to 4-Mepy vapour.

In the case of pym, the vapour exposure provided an unknown pattern was obtained by the vapour exposure shown in (b). However, essentially the same pattern as that of complex 3 was obtained by drying the sample as shown (c).

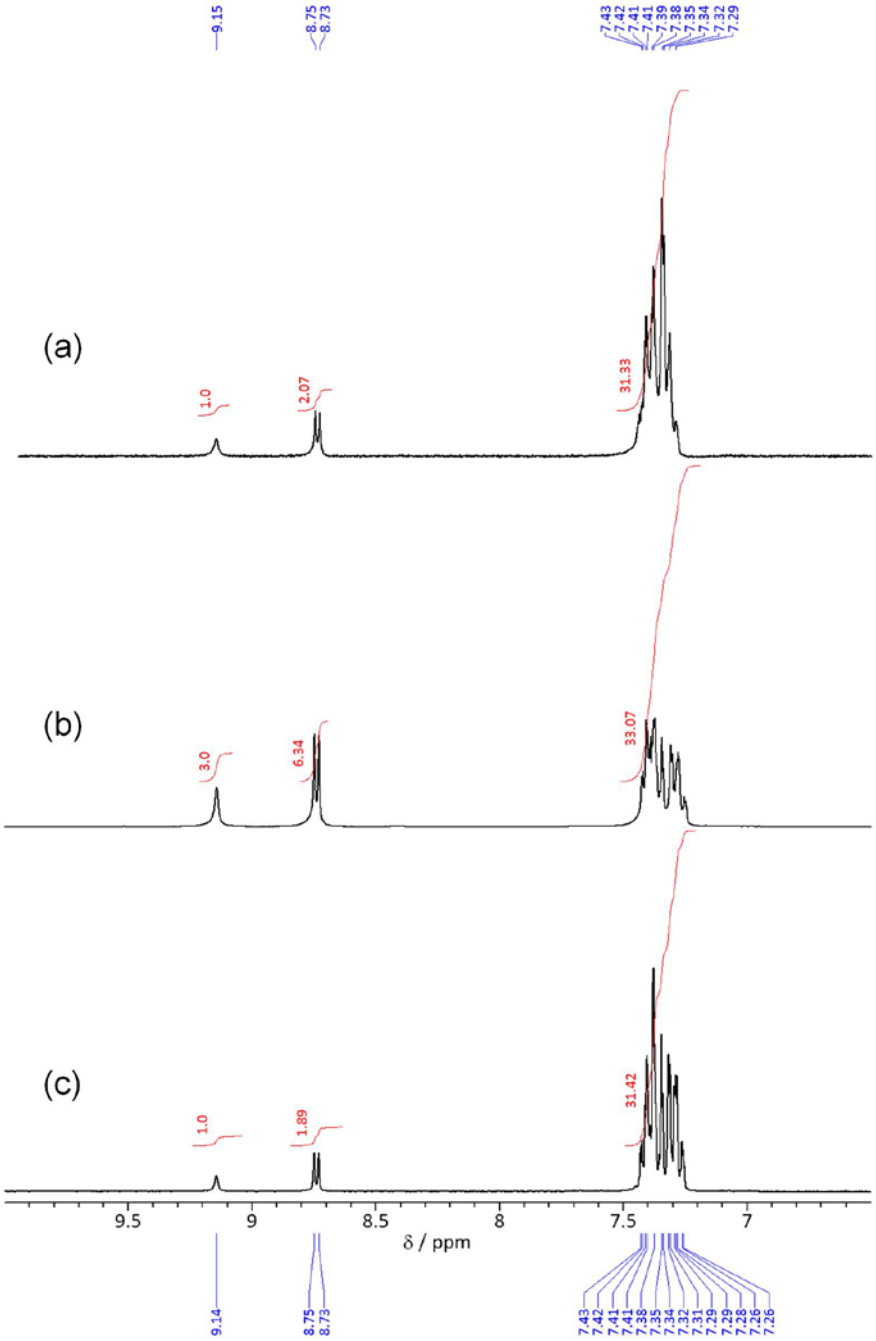

Fig. S2. Aromatic regions in ^{1}H NMR spectra (CD_3CN); (a) the crystalline sample of **3**, (b) the sample prepared by pym vapour exposure, and (c) the sample after drying under vacuum. The integrated values in (b) suggested that the two pym molecules are included in the crystal except for one coordinated pym molecule.

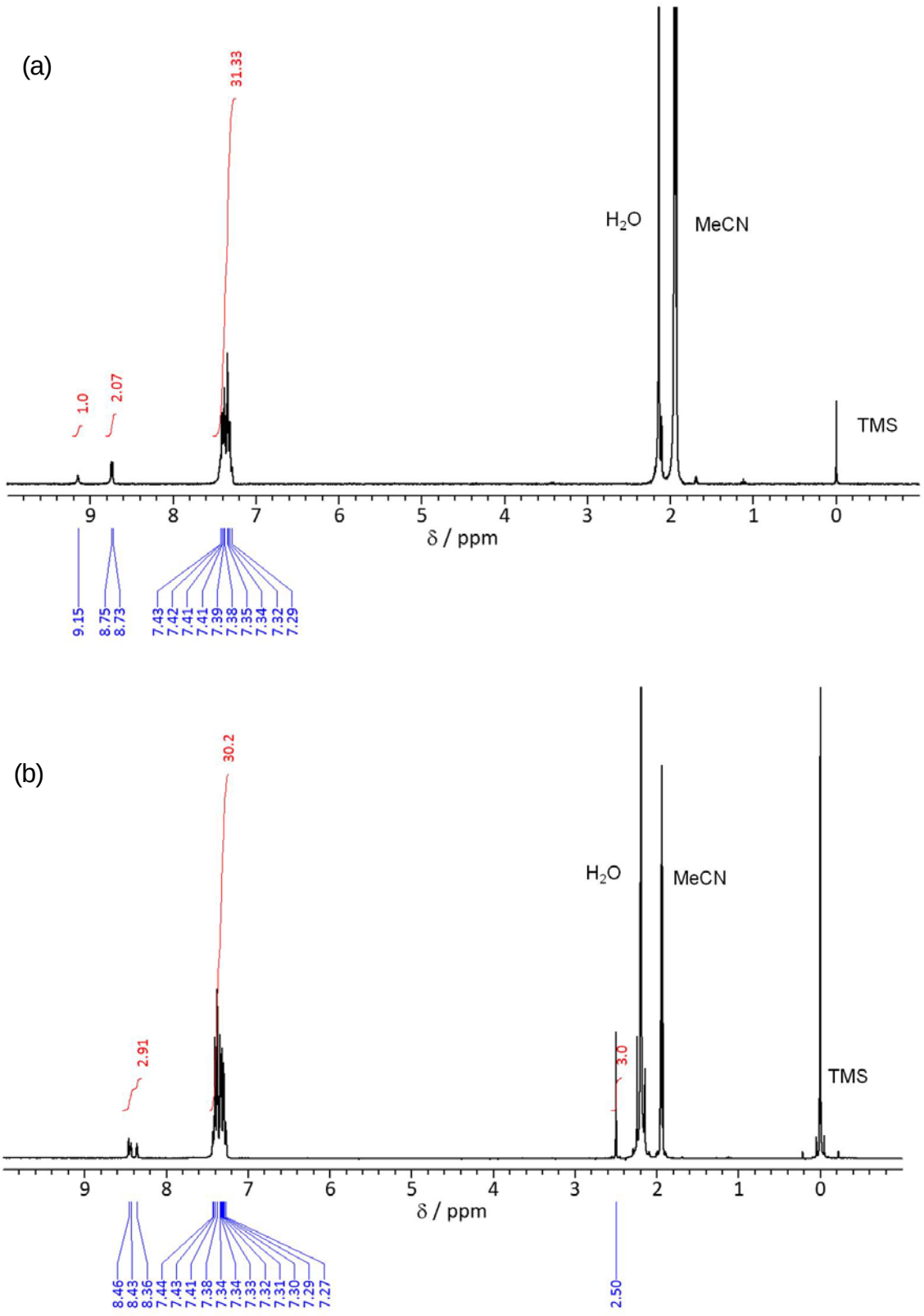

Fig. S3. ^{1}H NMR spectra (in CD_3CN) of crystalline sample for (a) **3** and (b) **4** (270 MHz).

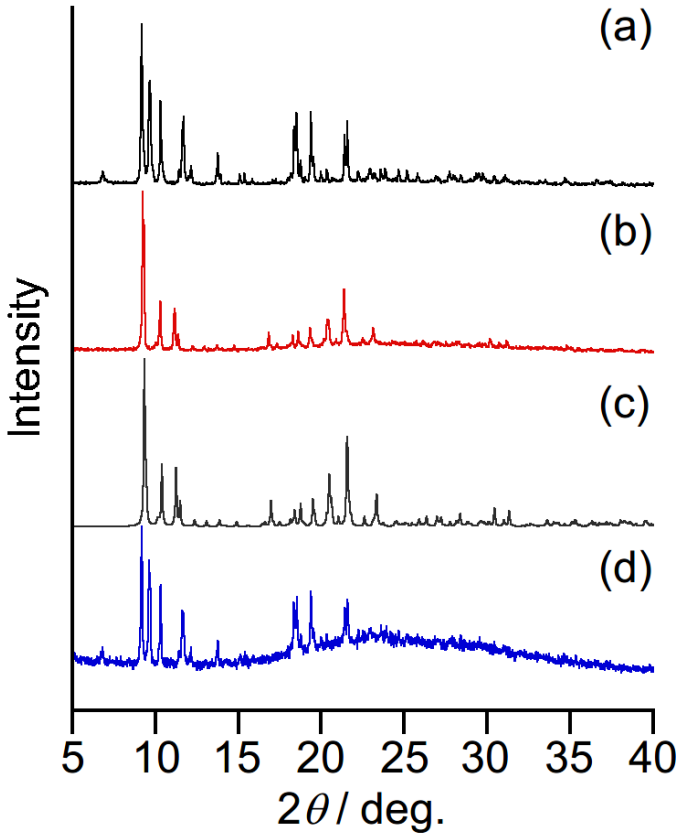

Fig. S4. Reversible PXRD pattern changes of complex **1**: (a) PXRD pattern of complex **1**, and (b) that after 2-Mepyz vapour exposure. (c) The simulation patterns of complex **4**, and PXRD pattern after exposing the sample (b) to 4-Mepy vapour.

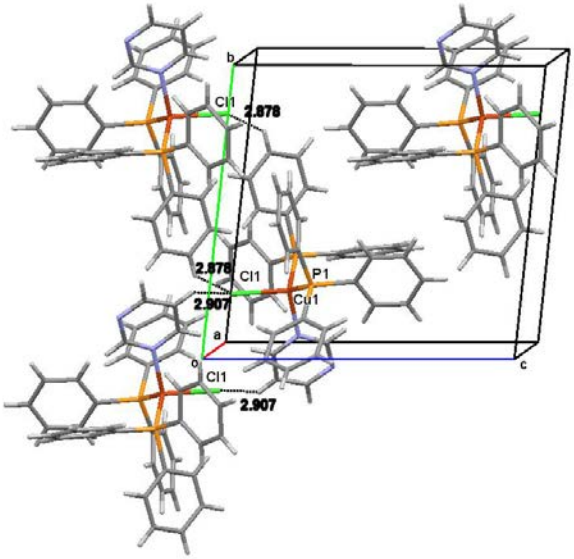

(a)

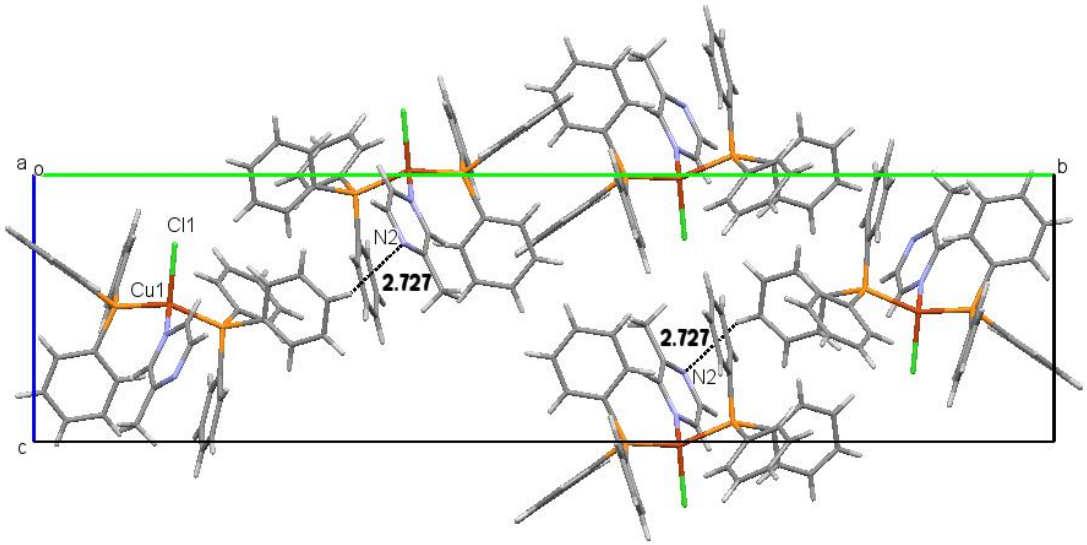

(b)

Fig. S5. Packing diagrams for (a) **3** and (b) **4** showing intermolecular short contacts.

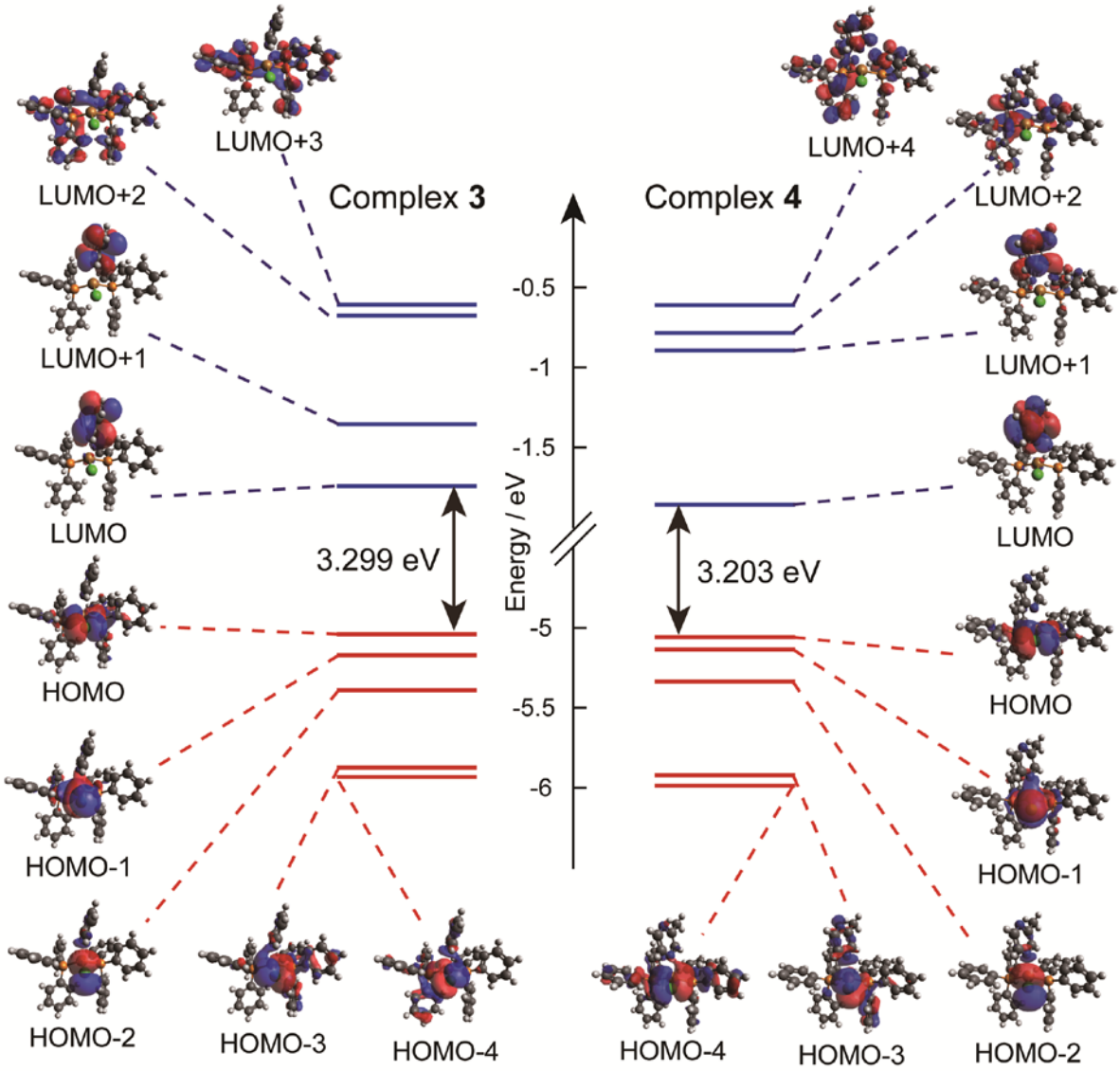

Fig. S6. Schematic molecular orbital diagrams and orbital shapes related to calculated transition of **3** and **4**. Molecular structure is determined by X-ray crystallographic analysis.

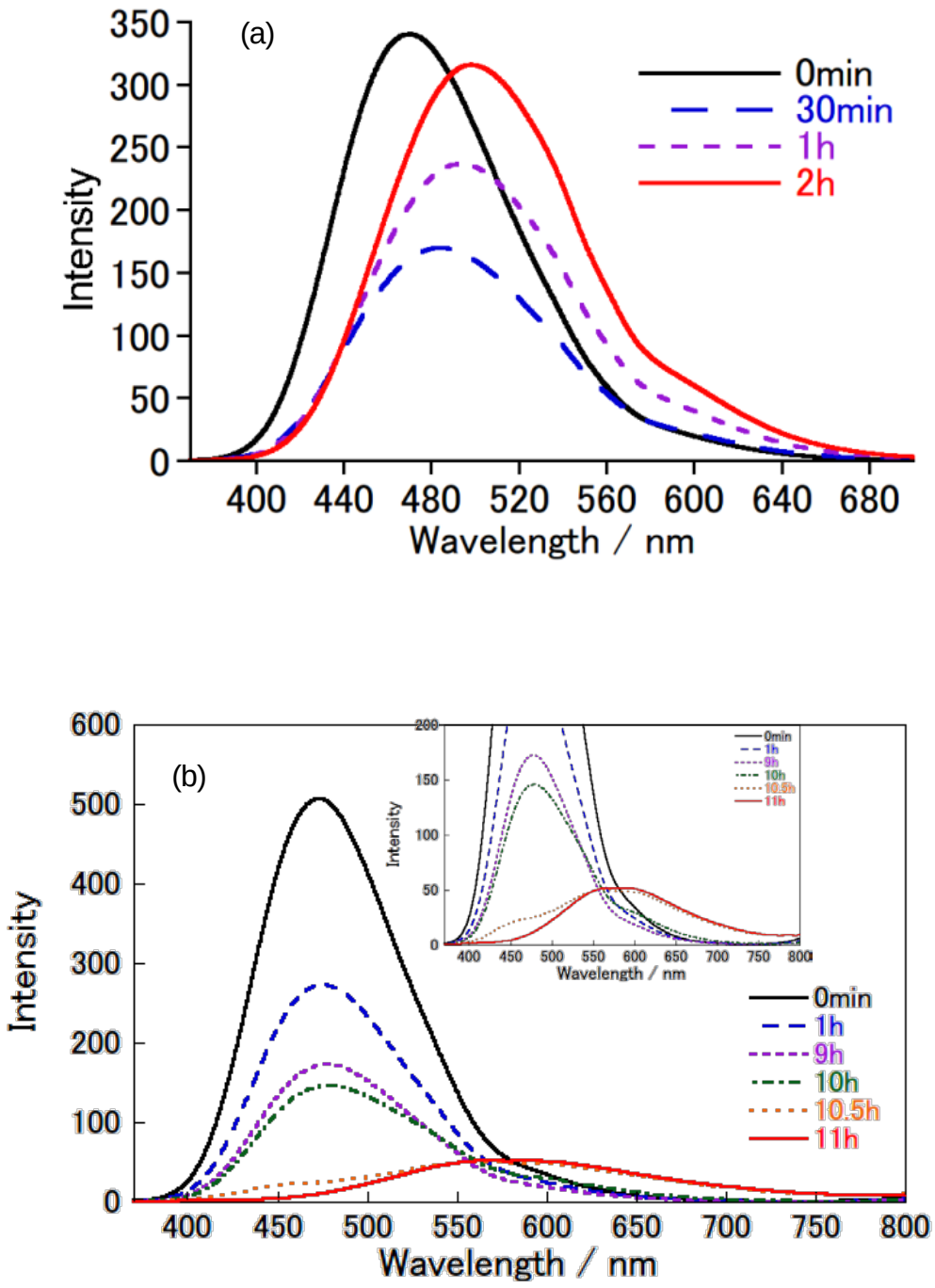

Fig. S7. Luminescence spectral change of complex **1** under exposure to py (a) and pym (b) vapour (λ_{ex} = 350 nm); inset: the enlarged drawings of (a) and (b)